Chemical Science

ROYAL SOCIETY OF CHEMISTRY

EDGE ARTICLE

View Article Online
View Journal | View Issue

Cite this: *Chem. Sci.*, 2022, **13**, 7536

All publication charges for this article have been paid for by the Royal Society of Chemistry

Received 4th May 2022
Accepted 2nd June 2022

DOI: 10.1039/d2sc02494b

rsc.li/chemical-science

Separation of pyrrolidine from tetrahydrofuran by using pillar[6]arene-based nonporous adaptive crystals†

Jiajun Cao, ‡[a] Yitao Wu,‡[a] Qi Li, [a] Weijie Zhu,[a] Zeju Wang,[a] Yang Liu,[a] Kecheng Jie, [a] Huangtianzhi Zhu *[a] and Feihe Huang *[abc]

Pyrrolidine, an important feedstock in the chemical industry, is commonly produced *via* vapor-phase catalytic ammoniation of tetrahydrofuran (THF). Obtaining pyrrolidine with high purity and low energy cost has extremely high economic and environmental values. Here we offer a rapid and energy-saving method for adsorptive separation of pyrrolidine and THF by using nonporous adaptive crystals of per-ethyl pillar[6]arene (**EtP6**). **EtP6** crystals show a superior preference towards pyrrolidine in 50 : 50 (v/v) pyrrolidine/THF mixture vapor, resulting in rapid separation. The purity of pyrrolidine reaches 95% in 15 min of separation, and after 2 h, the purity is found to be 99.9%. Single-crystal structures demonstrate that the selectivity is based on the stability difference of host–guest structures after uptake of THF or pyrrolidine and non-covalent interactions in the crystals. Besides, **EtP6** crystals can be recycled efficiently after the separation process owing to reversible transformations between the guest-free and guest-loaded **EtP6**.

Pyrrolidine is an important feedstock in the chemical industry that has been widely used in the production of food, pesticides, daily chemicals, coatings, textiles, and other materials.[1] Particularly, pyrrolidine is a raw material for organic synthesis of medicines such as buflomedil, pyrrocaine, and prolintane.[2] Moreover, pyrrolidine is also used as a solvent in the semi-synthetic process of simvastatin, one of the best-selling cardiovascular drugs.[3] In the chemical industry, there are many preparation methods for pyrrolidine. The most common way to obtain pyrrolidine is the gas-phase catalytic method using tetrahydrofuran (THF) and ammonia as raw materials;[4] this is carried out at high temperature under catalysis by solid acids. However, separating pyrrolidine from the crude product is difficult because of similar molecular weights and structures between pyrrolidine (b.p. 360 K and saturated vapor pressure = 1.8 kPa at 298 K) and THF (b.p. 339 K and saturated vapor pressure = 19.3 kPa at 298 K), which result in complicated processes and large energy consumption.[5] Therefore, it is worthwhile to find energy-efficient and simple methods to separate pyrrolidine from THF.

Many techniques and materials, including porous zeolites, metal–organic frameworks (MOFs), and porous polymers, have facilitated energy-efficient separations of important petrochemicals and feedstocks, including THF and pyrrolidine.[6,7] However, some drawbacks of these materials cannot be ignored.[8] For example, the relatively low thermal and moisture stabilities of MOFs limit their practical applications. Therefore, the development of new materials with satisfactory chemical and thermal stabilities for pyrrolidine/THF separation is of high significance.

In the past decade, pillararenes have been widely studied in supramolecular chemistry.[9] Owing to their unique pillar structures and diverse host–guest recognitions, pillararenes have been used in the construction of numerous supramolecular systems.[10] Recently, nonporous adaptive crystals (NACs) of macrocycles, which have shown extraordinary performance in adsorption and separation, have been developed by our group as a new type of adsorption and separation materials.[11] Unlike MOFs, covalent-organic frameworks (COFs), and other materials with pre-existing pores, NACs do not have "pores" in the guest-free form, whereas they adsorb guest vapors through cavities of macrocycles and spaces between macrocycles. NACs have been applied in separations of many significant chemicals such as alkane isomers, aromatics, and halohydrocarbon isomers.[12] However, such materials have never been used to

[a]*State Key Laboratory of Chemical Engineering, Stoddart Institute of Molecular Science, Department of Chemistry, Zhejiang University, Hangzhou 310027, PR China. E-mail: htzzhu@zju.edu.cn; fhuang@zju.edu.cn; Fax: +86-571-8795-3189; Tel: +86-571-8795-3189*

[b]*ZJU-Hangzhou Global Scientific and Technological Innovation Center, Hangzhou 311215, PR China*

[c]*Green Catalysis Center and College of Chemistry, Zhengzhou University, Zhengzhou 450001, PR China*

† Electronic supplementary information (ESI) available. CCDC 2132121–2132123. For ESI and crystallographic data in CIF or other electronic format see https://doi.org/10.1039/d2sc02494b

‡ Jiajun Cao and Yitao Wu are first co-authors.

separate pyrrolidine and THF. Herein, we utilized pillararene crystals as a separation material and realized the selective separation of pyrrolidine from a mixture of pyrrolidine and THF. We found that nonporous crystals of per-ethyl pillar[6]arene (**EtP6**) exhibited a shape-sorting ability at the molecular level towards pyrrolidine with an excellent preference, while crystals of per-ethyl pillar[5]arene (**EtP5**) did not (Scheme 1). In-depth investigations revealed that the separation was driven by the host–guest complexation between pyrrolidine and **EtP6**, which resulted in the formation of a more stable structure upon adsorption of pyrrolidine vapor in the crystalline state. **EtP6** crystals can also adsorb THF. However, when these two chemicals simultaneously exist as the vapor of a 50 : 50 (v/v) mixture, **EtP6** prefers pyrrolidine as an adsorption target. Compared with previously reported NAC-based separation, this separation took place rapidly. 95% purity was achieved in 15 min, and the purity increased to 99.9% after 2 h of separation. Moreover, pyrrolidine was removed upon heating, along with the structural transformation of **EtP6** back to its original state, endowing **EtP6** with excellent recyclability.

EtP5 and **EtP6** were prepared as previously described and then a pretreatment process was carried out to obtain guest-free **EtP5** and **EtP6** (Fig. S1–S4†).[13] According to powder X-ray diffraction (PXRD) patterns, activated **EtP5** and **EtP6** (denoted as **EtP5**α and **EtP6**β, respectively) were crystalline, and the patterns matched previous reports (Fig. S5 and S6†).[14] Studies from our group indicated that **EtP5**α and **EtP6**β crystals were nonporous, presumably due to their dense packing modes.

We first investigated the adsorption capabilities of **EtP5**α and **EtP6**β towards pyrrolidine and THF vapors. Based on time-dependent solid–vapor adsorption procedures, both **EtP5**α and **EtP6**β showed good ability to adsorb pyrrolidine and THF vapors. As shown in Fig. 1a, the adsorption amount of THF in **EtP5**α was higher than that of pyrrolidine. It took 6 hours for **EtP5**α to reach saturation points for adsorption of both pyrrolidine and THF vapors. The final storage of THF in **EtP5**α was 2 : 1 (molar ratio to the host), whereas the storage of pyrrolidine was 1 : 1. It seemed that the THF vapor was favored to occupy **EtP5**α, which was ascribed to the relatively lower boiling point of THF. A similar phenomenon was found for **EtP6**β. Time-dependent solid–vapor adsorption experiments for pyrrolidine demonstrated that it took just 1 hour to reach the saturation point, while it took 4 hours for the THF vapor (Fig. 1b). The adsorption amount of THF vapor was twice that of pyrrolidine.

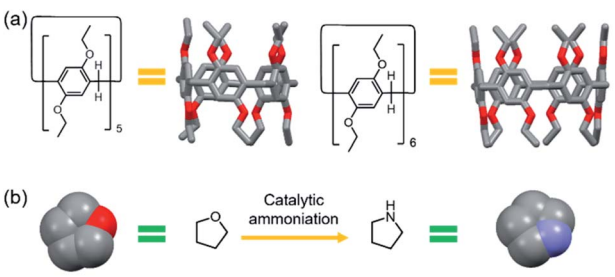

Scheme 1 Chemical structures and cartoon representations: (a) **EtP5** and **EtP6**; (b) THF and pyrrolidine.

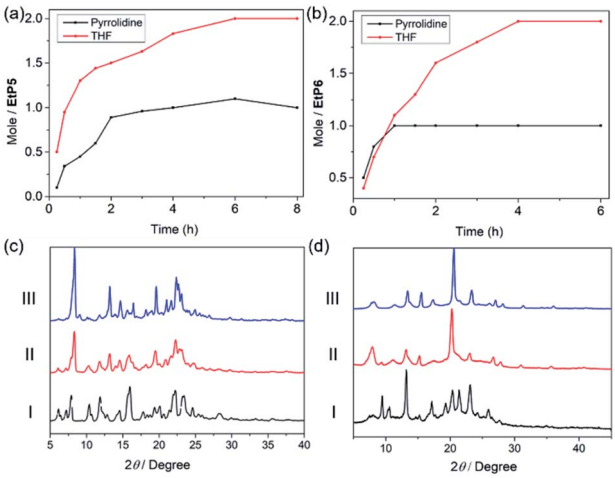

Fig. 1 Time-dependent solid–vapor adsorption plots of (a) **EtP5**α and (b) **EtP6**β for single-component pyrrolidine and THF vapors. PXRD patterns of (c) **EtP5**α and (d) **EtP6**β: (I) original activated crystals; (II) after adsorption of THF vapor; (III) after adsorption of pyrrolidine vapor.

^{1}H NMR spectra and thermogravimetric analyses (TGA) further confirmed the adsorption and storage of THF and pyrrolidine in both hosts (Fig. S7–S16†). Meanwhile, in the desorption process, adsorbed pyrrolidine and THF in **EtP6**β were easily released under reduced pressure and heating. Based on these data, it was clear that pyrrolidine could be adsorbed rapidly by both **EtP5**α and **EtP6**β in molar ratios = 1 : 1, while THF could be captured in a relatively slow process. Structural changes after adsorption of these two vapors were analyzed *via* PXRD experiments, in which varying degrees of changes before and after adsorption were observed, evidencing the appearance of new crystal structures (Fig. 1c and d). Nevertheless, only slight differences were observed in the PXRD patterns after the adsorption of THF or pyrrolidine, which might be ascribed to the structural similarity of the two molecules.

To study the mechanism of adsorption, guest-loaded single crystals were obtained by slowly evaporating either THF or pyrrolidine solutions of pillararenes (Tables S2 and S3†). In the

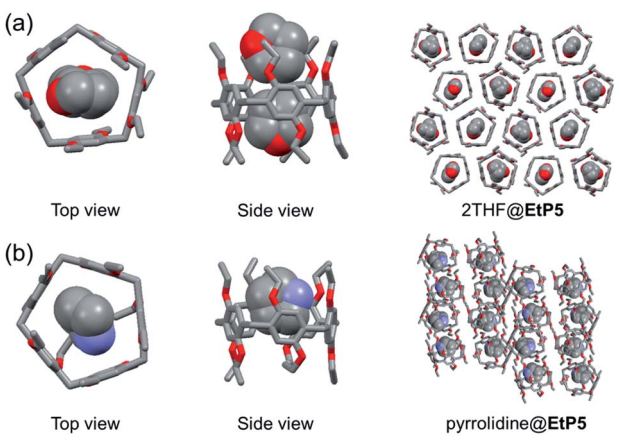

Fig. 2 Single crystal structures: (a) 2THF@**EtP5**; (b) pyrrolidine@**EtP5**.

crystal structure of THF-loaded **EtP5** (2THF@**EtP5**, Fig. 2a and S17†),[11a] two THF molecules are in the cavity of one **EtP5** molecule driven by multiple C–H···O hydrogen bonds and C–H···π bonds. **EtP5** assembles into honeycomb-like infinite edge-to-edge 1D channels. In the crystal structure of pyrrolidine-loaded **EtP5** (pyrrolidine@**EtP5**, Fig. 2b and S19†), one pyrrolidine molecule, stabilized by C–H···π interactions and C–H···O hydrogen bonds between hydrogen atoms on pyrrolidine and oxygen atoms on **EtP5**, is found in the cavity of **EtP5**. It's worth mentioning that a hydrogen atom which is linked with the N atom of pyrrolidine also forms a strong hydrogen bond with an oxygen atom on the ethoxy group of **EtP5**. **EtP5** forms imperfect 1D channels because of partial distortion of orientation. The PXRD patterns simulated from these crystal structures matched well with the experimental results (Fig. S18 and S20†), which verified that the uptake of vapors transformed **EtP5**α into pyrrolidine-loaded **EtP5**.

In the crystal structure of THF-loaded **EtP6** (2THF@**EtP6**, Fig. 3a and S21†), one **EtP6** molecule encapsulated two THF molecules in its cavity with C–H···O interactions, forming a 1 : 2 host–guest complex. Although 1D channels are observed, **EtP6** adopts a slightly different conformation, caused by the presence of THF. Moreover, the PXRD pattern of **EtP6**β after adsorption of THF vapor matches well with that simulated from 2THF@**EtP6**, which is evidence for the structural transformation upon adsorption. In the crystal structure of pyrrolidine-loaded **EtP6** (pyrrolidine@**EtP6**, Fig. 3b and S23†), a 1 : 1 host–guest complex with pyrrolidine is found. Driven by C–H···π interactions and C–H···O hydrogen bonds formed by hydrogen atoms on pyrrolidine and oxygen atoms on **EtP6**, one pyrrolidine molecule is in the cavity of **EtP6** with the nitrogen atom inside the cavity. The window-to-window packing mode of hexagonal **EtP6** molecules in pyrrolidine@**EtP6** contributes to the formation of honeycomb-like infinite edge-to-edge 1D channels, favorable for guest adsorption. Likewise, the PXRD result of **EtP6**β after adsorption of pyrrolidine is in line with the simulated pattern of pyrrolidine@**EtP6**, indicating that **EtP6**β transformed into pyrrolidine@**EtP6** in the presence of pyrrolidine (Fig. S22 and S24†).

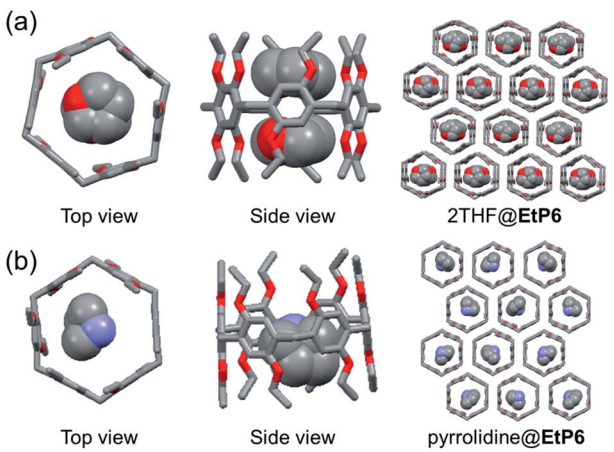

Fig. 3 Single crystal structures: (a) 2THF@**EtP6**; (b) pyrrolidine@**EtP6**.

According to the adsorption ability and different crystal structures after adsorption of guest vapors, we wondered whether **EtP5**α or **EtP6**β could separate mixtures of THF and pyrrolidine. We first evaluated separation by **EtP5**α. GC analysis indicated that the adsorption ratios of THF and pyrrolidine were 65.7% and 34.3%, respectively, when **EtP5**α was exposed to 50 : 50 (v/v) pyrrolidine/THF mixture vapor (Fig. 4a and S25†). Such adsorption was also illustrated by ^{1}H NMR (Fig. S26†). Although **EtP5**α showed a preference for THF, the selectivity is not satisfactory and cannot be applied to industrial separation. The less satisfactory selectivity may be ascribed to the similar crystal structures of **EtP5** after adsorption of THF or pyrrolidine and insufficient strong stabilizing interactions. The PXRD pattern of **EtP5**α after adsorption of the 50 : 50 (v/v) pyrrolidine/THF mixture vapor exhibited minor differences compared with that simulated from either 2THF@**EtP5** or pyrrolidine@**EtP5**, due to poor selectivity (Fig. 4b).

Nevertheless, selective separation of THF and pyrrolidine was achieved with **EtP6**β. As shown in Fig. 4c, time-dependent solid–vapor adsorption experiments for a 50 : 50 (v/v) pyrrolidine/THF mixture were conducted. Unlike the phenomenon in single-component adsorption experiments, uptake of pyrrolidine by **EtP6**β increased and reached the saturation point rapidly (less than 2 hours), while capture of THF was negligible. According to the NMR and GC results (Fig. S27 and S28†), the purity of pyrrolidine was determined to be 99.9% after 2 hours of adsorption, which indicates the remarkable selectivity of **EtP6**β for pyrrolidine. The PXRD pattern of **EtP6**β after adsorption of the mixture was

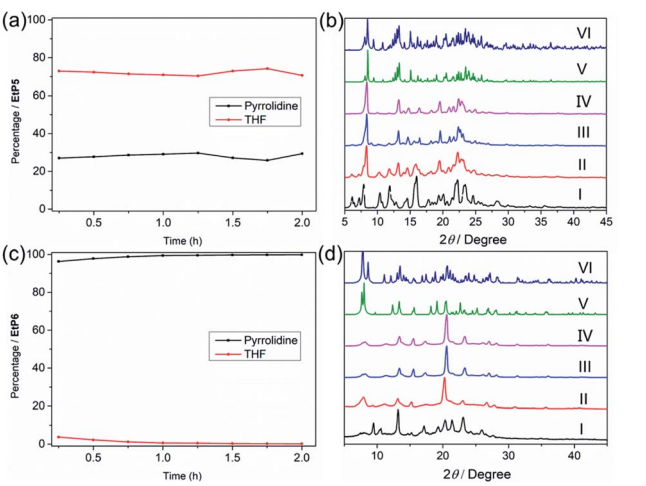

Fig. 4 (a)Time-dependent solid–vapor adsorption plot for **EtP5**α in the presence of 50 : 50 (*v*/*v*) pyrrolidine/THF mixture vapor. (b) PXRD patterns of **EtP5**α: (I) original **EtP5**α; (II) after adsorption of THF vapor; (III) after adsorption of pyrrolidine vapor; (IV) after adsorption of pyrrolidine/THF mixture vapor; (V) simulated from the single crystal structure of pyrrolidine@**EtP5**α; (VI) simulated from the single crystal structure of 2THF@**EtP5**α. (c) Time-dependent solid–vapor adsorption plot for **EtP6**β in the presence of 50 : 50 (v/v) pyrrolidine/THF mixture vapor. (d) PXRD patterns of **EtP6**β: (I) original **EtP6**β; (II) after adsorption of THF vapor; (III) after adsorption of pyrrolidine vapor; (IV) after adsorption of pyrrolidine/THF mixture vapor; (V) simulated from the single crystal structure of pyrrolidine@**EtP6**β; (VI) simulated from the single crystal structure of 2THF@**EtP6**β.

consistent with that from single-component adsorption, indicating the structural transformation in the crystalline state upon selective capture of pyrrolidine from the mixture. Although THF and pyrrolidine have similar molecular structures, their non-covalent interactions with **EtP6** are different. We assume that the hydrogen bond between N–H and the oxygen atom on **EtP6** stabilizes pyrrolidine and leads to such selectivity. More importantly, compared with previous adsorption processes using NACs reported by our group, the selective separation of pyrrolidine was completed rapidly. According to the GC results, the purity of pyrrolidine reached around 95% in the initial 15 min, while it usually takes hours for selective separations of other substrates using NACs. Increasing the adsorption time to 2 h improves the purity to over 99%. The rapid separation of pyrrolidine with high purity using **EtP6**β shows great potential in industrial applications.

Apart from selectivity, recyclability is also an important parameter for an adsorbent. Consequently, recycling experiments were carried out by heating pyrrolidine@**EtP6** under vacuum at 100 °C to remove adsorbed pyrrolidine. According to TGA and PXRD analysis, the recycled **EtP6** solid maintained crystallinity and structural integrity that were the same as those of activated **EtP6** crystals (Fig. S29 and S30†). Besides, it is worth mentioning that the recycled **EtP6** solids were still capable of separating mixtures of pyrrolidine and THF without loss of performance after being recycled five times (Fig. S31†).

In conclusion, we explored the separation of pyrrolidine/THF mixtures using NACs of **EtP5** and **EtP6**. Pyrrolidine was purified using **EtP6** from a 50 : 50 (v/v) pyrrolidine/THF mixture with a purity of 99.9%, but **EtP5** exhibited selectivity towards THF. Moreover, the separation of pyrrolidine by **EtP6** was extremely fast so that over 95% purity was determined within 15 min of adsorption. The rapid separation is unique among NAC-based separations. Single-crystal structures revealed that the selectivity depended on the stability of the new structures after adsorption of the guests and the non-covalent interactions in the host–guest complexes. PXRD patterns indicated that the structures of the host crystals changed into the host–guest complexes after adsorption. Additionally, the NACs of **EtP6** exhibited excellent recyclability over at least five runs; this endows **EtP6** with great potential as an alternative adsorbent for rapid purification of pyrrolidine that can be applied in practical industry. The fast separation with such simple NACs in this work also reveals that minor structural differences can cause significant changes in properties, which should provide perspectives on designs of adsorbents or substrates with specifically tailored binding sites.

Data availability

The crystallographic data for pyrrolidine@**EtP5**, 2THF@**EtP6** and pyrrolidine@**EtP6** have been deposited at CCDC with deposition numbers 2132121, 2132122 and 2132123, respectively.

Author contributions

J. C., Z. H. and F. H. proposed the project and designed the study, J. C. and Y. W. performed the experiments, J. C., Q. L., Z. W., Y. L. and W. Z. analyzed the data. J. C. and Y. W. wrote the manuscript with inputs from all authors. F. H. directed the project with critical consultation from H. Z. and K. J.

Conflicts of interest

There are no conflicts to declare.

Acknowledgements

F. H. thanks the National Key Research and Development Program of China (2021YFA0910100), National Natural Science Foundation of China (22035006), Zhejiang Provincial Natural Science Foundation of China (LD21B020001) and the Starry Night Science Fund of Zhejiang University Shanghai Institute for Advanced Study (SN-ZJU-SIAS-006) for financial support.

Notes and references

1 X. Wen, *Appl. Chem. Ind.*, 2007, **36**, 913.
2 S. P. Clissold, S. Lynch and E. M. Sorkin, *Drugs*, 1987, **33**, 430.
3 (*a*) S. Zhao, W. Xu and J. Zhao, *Acta Pet. Sin.*, 2012, **28**, 127; (*b*) D. Saffles, D. F. Lawson and M. Stayer, EP 0626278, 1994; (*c*) N. Yoshiyana, JP 04133275, 1992; (*d*) S. Furukawa, JP 4137362, 1992.
4 (*a*) K. Fujita, K. Hatada and Y. Ono, *J. Catal.*, 1974, **35**, 325; (*b*) K. Hatada, M. Shimada and K. Fujita, *J. Catal.*, 1974, **35**, 439.
5 (*a*) V. Yarlagadda, S. Rao, S. J. Kulkarni, M. Suvrahmanyam and A. V. Rama Rao, *J. Org. Chem.*, 1994, **59**, 3998; (*b*) C. Tsung, J. N. Kuhn, W. Huang, C. Aliaga, L.-I. Hung, G. A. Somorjai and P. Yang, *J. Am. Chem. Soc.*, 2009, **131**, 5816.
6 C.-X. Yang and X.-P. Yan, *Anal. Chem.*, 2011, **83**, 7144.
7 (*a*) M. Lippi and M. Cametti, *Coord. Chem. Rev.*, 2021, **430**, 213661; (*b*) Q. Zhang, Y. Cui and G. Qian, *Coord. Chem. Rev.*, 2019, **378**, 310.
8 (*a*) M. Eddaoudi, H. Li and O. M. Yaghi, *J. Am. Chem. Soc.*, 2000, **122**, 1391; (*b*) A. Kirchon, L. Feng, H. F. Drake, E. A. Joseph and H.-C. Zhou, *Chem. Soc. Rev.*, 2018, **47**, 8611; (*c*) O. M. Yaghi, H. Li, C. Davis, D. Richardson and T. L. Groy, *Acc. Chem. Res.*, 1998, **31**, 474; (*d*) Y. Bai, Y. Dou, L. H. Xie, W. Rutledge, J.-R. Li and H.-C. Zhou, *Chem. Soc. Rev.*, 2016, **45**, 2327; (*e*) D. F. Sava, K. W. Chapman, M. A. Rodriguez, J. A. Greathouse, P. S. Crozier, H.-Y. Zhao, P. J. Chupas and T. M. Nenoff, *Chem. Mater.*, 2013, **25**, 2591; (*f*) X. Zhao, X. Bu, E. T. Nguyen, Q.-G. Zhai, C. Mao and P. Feng, *J. Am. Chem. Soc.*, 2016, **138**, 15102.
9 (*a*) T. Ogoshi, S. Kanai, S. Fujinami, T. Yamagishi and Y. Nakamoto, *J. Am. Chem. Soc.*, 2008, **130**, 5022; (*b*) M. Xue, Y. Yang, X. Chi, Z. Zhang and F. Huang, *Acc. Chem. Res.*, 2012, **45**, 1294; (*c*) B. Li, Z. Meng, Q. Li, X. Huang, Z. Kang, H. Dong, J. Chen, J. Sun, Y. dong, J. Li, X. Jia, J. L. Sessler, Q. Meng and C. Li, *Chem. Sci.*, 2017, **8**, 4458; (*d*) T. Ogoshi, T.-a. Yamagishi and Y. Nakamoto, *Chem. Rev.*, 2016, **116**, 7937; (*e*) H. Zhu, Q. Li, B. Shi, H. Xing, Y. Sun, S. Lu, L. Shangguan, X. Li, F. Huang and P. J. Stang, *J. Am. Chem. Soc.*, 2020, **142**, 17340; (*f*) J.-R. Wu,

A. U. Mu, B. Li, C.-Y. Wang, L. Fang and Y.-W. Yang, *Angew. Chem., Int. Ed.*, 2018, **57**, 9853; (*g*) X.-N. Han, Y. Han and C.-F. Chen, *J. Am. Chem. Soc.*, 2020, **142**, 8262; (*h*) L.-L. Tan, H. Li, Y. Tao, S. X.-A. Zhang, B. Wang and Y.-W. Yang, *Adv. Mater.*, 2014, **26**, 7027; (*i*) N. L. Strutt, D. Fairen-Jimenez, J. Iehl, M. B. Lalonde, R. Q. Snurr, O. K. Farha, J. T. Hupp and J. F. Stoddart, *J. Am. Chem. Soc.*, 2012, **134**, 17436; (*j*) W. Si, Z.-T. Li and J.-L. Hou, *Angew. Chem., Int. Ed.*, 2014, **53**, 4578; (*k*) W. Si, P. Xin, Z.-T. Li and J.-L. Hou, *Acc. Chem. Res.*, 2015, **48**, 1612; (*l*) M. Mastalerz, *Acc. Chem. Res.*, 2018, **51**, 2411; (*m*) X.-Y. Hu, K. Jia, Y. Cao, Y. Li, S. Qin, F. Zhou, C. Lin, D. Zhang and L. Wang, *Chem.–Eur. J.*, 2015, **21**, 1208; (*n*) J.-R. Wu, Z. Cai, G. Wu, D. Dai, Y.-Q. Liu and Y.-W. Yang, *J. Am. Chem. Soc.*, 2021, **48**, 20395.

10 (*a*) C. Li, X. Shu, J. Li, J. Fan, Z. Chen, L. Weng and X. Jia, *Org. Lett.*, 2012, **14**, 4126; (*b*) X. Shu, W. Chen, D. Hou, Q. Meng, R. Zheng and C. Li, *Chem. Commun.*, 2014, **50**, 4820; (*c*) M. Zhang, P.-P. Zhu, P. Xin, W. Si, Z.-T. Li and J.-L. Hou, *Angew. Chem., Int. Ed.*, 2017, **56**, 2999; (*d*) Q. Duan, Y. Cao, Y. Li, X. Hu, T. Xiao, C. Lin, Y. Pan and L. Wang, *J. Am. Chem. Soc.*, 2013, **135**, 10542; (*e*) Y. Cao, X.-Y. Hu, Y. Li, X. Zou, S. Xiong, C. Lin, Y.-Z. Shen and L. Wang, *J. Am. Chem. Soc.*, 2014, **136**, 10762; (*f*) Q. Li, H. Zhu and F. Huang, *Trends Chem.*, 2020, **2**, 850; (*g*) S.-H. Li, H.-Y. Zhang, X. Xu and Y. Liu, *Nat. Commun.*, 2015, **6**, 7590; (*h*) M. Ni, N. Zhang, W. Xia, X. Wu, C. Yao, X. Liu, X.-Y. Hu, C. Lin and L. Wang, *J. Am. Chem. Soc.*, 2016, **138**, 6643.

11 (*a*) K. Jie, M. Liu, Y. Zhou, M. Little, S. Bonakala, S. Chong, A. Stephenson, L. Chen, F. Huang and A. I. Cooper, *J. Am. Chem. Soc.*, 2017, **139**, 2908; (*b*) T. Ogoshi, R. Sueto, K. Yoshikoshi, Y. Sakata, S. Akine and T.-a. Yamagishi, *Angew. Chem., Int. Ed.*, 2015, **54**, 9849; (*c*) T. Ogoshi, K. Saito, R. Sueto, R. Kojima, Y. Hamada, S. Akine, A. M. P. Moeljadi, H. Hirao, T. Kakuta and T.-a. Yamagishi, *Angew. Chem., Int. Ed.*, 2018, **57**, 1592; (*d*) Y. Wu J. Zhou, E. Li, M. Wang, K. Jie, H. Zhu and F. Huang, *J. Am. Chem. Soc.*, 2020, **142**, 19722; (*e*) A. Dey, S. Chand, B. Maity, P. M. Bhatt, M. Ghosh, L. Cavallo, M. Eddaoudi and N. M. Khashab, *J. Am. Chem. Soc.*, 2021, **143**, 4090; (*f*) J.-R. Wu and Y.-W. Yang, *Angew. Chem., Int. Ed.*, 2021, **60**, 1690; (*g*) J. L. Atwood, L. J. Barbour, A. Jerga and B. L. Schottel, *Science*, 2002, **298**, 1000; (*h*) P. K. Thallapally, B. P. McGrail, S. J. Dalgarno, H. T. Schaef, J. Tian and J. L. Atwood, *Nat. Mater.*, 2008, **7**, 146; (*i*) K. Jie, M. Liu, Y. Zhou, M. A. Little, A. Pulido, S. Y. Chong, A. Stephenson, A. R. Hughes, F. Sakakibara, T. Ogoshi, F. Blanc, G. M. Day, F. Huang and A. I. Cooper, *J. Am. Chem. Soc.*, 2018, **140**, 6921; (*j*) J.-R. Wu and Y.-W. Yang, *J. Am. Chem. Soc.*, 2019, **141**, 12280; (*k*) X. Sheng, E. Li, Y. Zhou, R. Zhao, W. Zhu and F. Huang, *J. Am. Chem. Soc.*, 2020, **142**, 6360; (*l*) X. Zhao, Y. Liu, Z.-Y. Zhang, Y. Wang, X. Jia and C. Li, *Angew. Chem., Int. Ed.*, 2021, **60**, 17904; (*m*) J.-R. Wu, B. Li, J.-W. Zhang and Y.-W. Yang, *ACS Appl. Mater. Interfaces*, 2019, **11**, 998; (*n*) J.-R. Wu, B. Li and Y.-W. Yang, *Small*, 2020, **16**, 2003490; (*o*) H.-Y. Zhou and C.-F. Chen, *Chem. Commun.*, 2022, **58**, 4356.

12 (*a*) J. Zhou, G. Yu, Q. Li, M. Wang and F. Huang, *J. Am. Chem. Soc.*, 2020, **142**, 2228; (*b*) M. Wang, J. Zhou, E. Li, Y. Zhou, Q. Li and F. Huang, *J. Am. Chem. Soc.*, 2019, **141**, 17102; (*c*) Q. Li, K. Jie and F. Huang, *Angew. Chem., Int. Ed.*, 2020, **59**, 5355; (*d*) Y. Zhao, H. Xiao, C.-H. Tung, L.-Z. Wu and H. Cong, *Chem. Sci.*, 2021, **12**, 15528; (*e*) K. Jie, Y. Zhou, E. Li and F. Huang, *Acc. Chem. Res.*, 2018, **51**, 2064; (*f*) Y. Wang, K. Xu, B. Li, L. Cui, J. Li, X. Jia, H. Zhao, J. Fang and C. Li, *Angew. Chem., Int. Ed.*, 2019, **58**, 10281; (*g*) H. Zuilhof, K. Samanta, W. Yang, X. Wan, T. U. Thikekar, Y. Chao, S. Li, K. Du, J. Xu, Y. Gao and A. C.-H. Sue, *Angew. Chem., Int. Ed.*, 2020, **59**, 3994; (*h*) H. Yao, Y.-M. Wang, M. Quan, M. U. Farooq, L.-P. Yang and W. Jiang, *Angew. Chem., Int. Ed.*, 2020, **59**, 19945; (*i*) D. Luo, J. Tian, J. L. Sessler and X. Chi, *J. Am. Chem. Soc.*, 2021, **143**, 18849; (*j*) Y. Zhou, K. Jie, R. Zhao, E. Li and F. Huang, *J. Am. Chem. Soc.*, 2020, **142**, 6957; (*k*) J.-R. Wu, B. Li and Y.-W. Yang, *Angew. Chem., Int. Ed.*, 2020, **59**, 2251; (*l*) Q. Li, H. Zhu and F. Huang, *J. Am. Chem. Soc.*, 2019, **141**, 13290; (*m*) J.-R. Wu and Y.-W. Yang, *CCS Chem.*, 2020, **2**, 836.

13 X.-B. Hu, Z. Chen, L. Zhang, J.-L. Hou and Z.-T. Li, *Chem. Commun.*, 2012, **48**, 10999.

14 K. Jie, Y. Zhou, E. Li, R. Zhao and F. Huang, *Angew. Chem., Int. Ed.*, 2018, **57**, 12845.